

Results from EXO–200

D.J. Auty on behalf of the EXO–200 Collaboration

Dep. of Physics and Astronomy, University of Alabama, 206 Gallalee Hall,
Tuscaloosa, AL 35487-0324, USA

E-mail: dauty@ua.edu

Abstract. EXO–200 is a double-beta decay experiment that measures the half-life of the decay of ^{136}Xe . This article describes the result reported by EXO–200 in the summer 2012, with an exposure of 32.5 kg-yr, saw no signal for the $0\nu\beta\beta$ decay. This sets a lower limit for the half-life of the neutrinoless double-beta decay $T_{1/2}^{0\nu\beta\beta}(^{136}\text{Xe}) > 1.6 \times 10^{25} \text{ yr}$ (90 % CL), which sets a limit on the Majorana neutrino mass, depending on which matrix element used, of 140 meV–380 meV.

1. Introduction

Several even-even nuclei are stable against ordinary β decay, but are unstable for $\beta\beta$ decay in which two neutrons are changed into two protons simultaneously. As is well known, $\beta\beta$ decay can proceed through several modes. The allowed process, the two-neutrino mode ($2\nu\beta\beta$), is completely described by known physics; its rate was first evaluated in [1]. Of the other, hypothetical, modes, the neutrino-less decay ($0\nu\beta\beta$) is forbidden in the Standard Model since it violates conservation of the total lepton number. EXO–200 is located at the Waste Isolation Pilot Plant (WIPP) in New Mexico, USA. EXO–200 uses xenon as both the $\beta\beta$ source and the detector of the summed electron energy. It uses 200 kg, of which 175 kg is in liquid phase, of xenon enriched to $(80.6 \pm 0.1)\%$ in the isotope ^{136}Xe . The remaining 19.4 % is ^{134}Xe , with other isotopes present only at low concentration. At operating temperature, 167 K, and a pressure, 147 kPa, the liquid xenon (LXe) has a density of 3.0 g cm^{-3} .

EXO-200 has been described in detail elsewhere [2]. Briefly, the detector is a cylindrical LXe time projection chamber (TPC), roughly 40 cm in diameter and 44 cm in length. Two drift regions are separated in the centre by a cathode. The TPC provides X-Y-Z coordinate and energy measurements of ionisation deposits in the LXe by simultaneously collecting the scintillation light and the charge. Charge deposits spatially separated by about 1 cm or more are individually observed and the position accuracy for isolated deposits is a few mm. Avalanche Photodiodes (APDs) measure the scintillation light. Small radioactive sources can be positioned at standard positions near the TPC to calibrate the detector and monitor its stability. The TPC is shielded from environmental radioactivity on all sides by ~ 50 cm of HFE-7000 cryofluid [3] maintained at ~ 167 K inside a vacuum-insulated copper cryostat. Further shielding is provided by at least 25 cm of lead in all directions. The entire assembly is housed underground in a cleanroom at a depth of 1585+11 meters water equivalent [4] at the Waste Isolation Pilot Plant near Carlsbad, NM, USA. Four of the six sides of the cleanroom are instrumented with plastic scintillator panels recording the passage of cosmic ray muons. An extensive materials screening campaign [5] was employed to minimise the radioactive background produced by the detector components.



2. Data

The active volume of the LXe for this analysis was the inner 98.5 kg LXe, 79.4 kg of ^{136}Xe . The data analysed was taken between 22nd September 2011 and 16th April 2012, for a total of 2896.6 live hours after cuts [6], which is 32.5 kg·yr livetime. Only events above 700 keV are included in this analysis, as this is where the trigger is 100 % efficient. Other analysis cuts that were used were: events in the TPC that happened 1 μs before or 25 ms after a veto panel triggered were rejected, making the veto efficiency $96.2^{+0.4}_{-3.7}\%$ at rejecting cosmic muons (0.58 % dead time); TPC events that happened within one second of each other to be rejected (3.3 % dead time), TPC events that happened within one minute after a muon was reconstructed in the TPC (5.0 % dead time), to reduce the daughter decays following the muon; alpha decays have a larger light to charge ratio than betas so were able to be cut on this. The total dead time due to the veto cuts was 8.6 %. The stability of the detector was achieved through daily calibrations mostly using the ^{228}Th source (2615 keV). A ^{60}Co (1173 keV and 1332 keV) and ^{137}Cs (662 keV) source were used less often to calibrate the energy for the full spectrum. The energy from an event can go into light and charge by various amounts, so smearing any peak out in either spectrum. We are able to use the known energy of the 2615 keV peak from ^{208}Tl decay to reduce the resolution by combine the light and charge by “rotating”, $E = S \sin \theta + I \cos \theta$, and fitting a Gaussian to the peak. Theta was varied to get the lowest width/mean for the fit. This improve the energy resolution compared to scintillation or charge only. The whole of the low background data was rotated with this theta, and the energy resolution parameterised as $\sigma^2 = a\sigma_e^2 + bE + E^2$ where σ_e^2 is the electronic noise contribution, bE is the statistical fluctuation in the ionisation and scintillation and cE^2 is the position and time dependant broadening. In the rotated energy spectrum at the Q-value the energy resolution was 1.67 % (1.84 %) SS (MS).

3. Analysis

The detectors ability to identify singlesite charge clusters (SS) and multi-site charge clusters (MS) events to distinguish between SS $\beta/\beta\beta$ events and MS γ events in the bulk xenon. The clustering resolution in two dimensions, U-dimension is 18 cm and 6 mm in z (drift time). The ability of the GEANT4 Monte Carlo (MC) to simulate the distributions for SS and MS energy spectra was proven on the ^{228}Th and ^{60}Co source data. The MC reproduces the fraction of SS events, defined as $N_{ss}/(N_{ss} + N_{ms})$ to $\pm 8.5\%$. The requirement that events be fully reconstructed¹ gives an efficiency of 70 % (71 %) for the ^{228}Th ($0\nu\beta\beta$) spectrum. The 71 % efficiency was further verified by comparing the $2\nu\beta\beta$ data spectrum with MC. ground Background models were generated for the various components of the detector from the material screening campaign, providing normalisation for the MC generated probability distribution functions (pdfs). These background contributions were estimated using previous generation of detector simulations [2], pdfs which account for <50 (<0.2) events in the $2\nu\beta\beta$ ($0\nu\beta\beta$) spectrum, were not included in the fit. The various generated pdfs were fitted to the data using a maximum likelihood fit and varied so that SS site events were constrained to be $\pm 8.5\%$ of the value predicted by the MC. As γ -rays were used to calibrate the detector, the energy of the β events was a free parameter in the fit, so it is constrained by the $2\nu\beta\beta$ events. The fit reports a scale factor of 0.995 ± 0.004 . The fit gives a expected background of $(1.5 \pm 0.1) \times 10^{-3} \text{ kg}^{-1} \text{ yr}^{-1} \text{ keV}^{-1}$ in the one sigma region of interest (ROI), where one sigma is 1.67 % of 2458 keV (41 keV), which is 3–4 events. Figure 1 shows that there is only one event in this region. The result from the fit is a $T_{1/2}^{0\beta\beta} > 1.6 \times 10^{25} \text{ yr}$ with the $T_{1/2}^{2\beta\beta} = 2.23 \pm 0.02$ (stat.) ± 0.22 (syst.) $\times 10^{21} \text{ yr}$. The dominate systematic errors are from the fiducial volume (12.34 %) and the β scale (9.32 %). $T_{1/2}^{0\beta\beta}$ can be converted into a limit on neutrino mass using various matrix elements which give a neutrino mass between 140 meV and 380 meV at 90 % CL. In Figure 2 the comparison between $T_{1/2}^{0\beta\beta}$ for

¹ have charge and scintillation signal

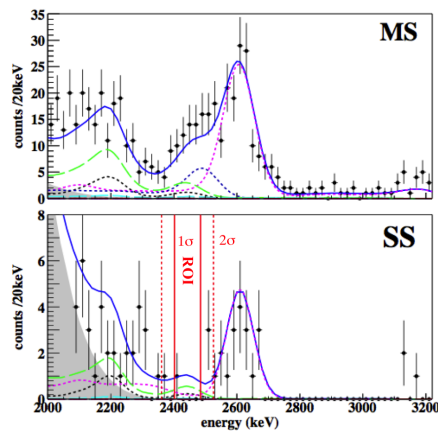


Figure 1. Energy spectra in the ^{136}Xe $Q_{\beta\beta}$ region for MS (top) and SS (bottom) events. The 1 (2) σ regions around $Q_{\beta\beta}$ are shown by solid (dashed) vertical lines. The best fit line (solid blue) is shown. The background components are $2\nu\beta\beta$ (grey region), ^{60}Co (dotted dark blue), ^{222}Rn in the cryostat-lead air-gap (long-dashed green), ^{238}U in the TPC vessel (dotted black), ^{232}Th in the TPC vessel (dotted magenta), ^{214}Bi on the cathode (long-dashed cyan), The $0\nu\beta\beta$ PDF from the fit is not visible.

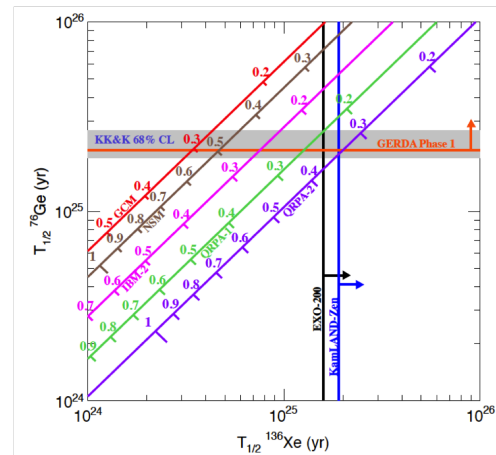


Figure 2. Relation between the $T_{1/2}^{0\nu\beta\beta}$ in ^{76}Ge and ^{136}Xe for different matrix element calculations (GCM [8], NSM [9], IBM-2 [10], RQRPA-1 [11] and QRPA-2 [12]). For each matrix element $\langle m \rangle_{\beta\beta}$ is also shown (eV). The claim [13] is represented by the grey band, along with the best limit for ^{76}Ge [14]. The result reported here is shown along with that from [7].

^{76}Ge and ^{136}Xe is shown with the predicted Majorana mass of the neutrino, also plotted are the limits set by this analysis and a previous analysis for KamLAND-Zen [7] for ^{136}Xe and the claimed observation and the 90% limit for ^{76}Ge . It can be seen that for most matrix elements the 90% limit from EXO is incompatible with the Ge observation. A new result released from EXO-200, after this poster was presented, using 99.8 kg-yr of ^{136}Xe has given a 90% CL $T_{1/2}^{0\nu} > 1.1 \cdot 10^{25}$ yr [15].

Acknowledgements

EXO-200 is supported by DoE and NSF in the United States, NSERC in Canada, SNF in Switzerland and RFBR in Russia. The collaboration gratefully acknowledges the WIPP for their hospitality

References

- [1] M. Goeppert-Mayer, *Phys. Rev.* **48**, 512 (1935).
- [2] M. Auger *et al.*, *JINST* **7**, P05010 (2012).
- [3] 3M HFE-7000, <http://www.3m.com/>.
- [4] E.I. Esch *et al.*, *Nucl. Instrum. Methods A* **538**, 516 (2005).
- [5] D.S. Leonard *et al.*, *Nucl. Instrum. Methods A* **591**, 490 (2008).
- [6] M. Auger *et al.*, *Phys. Rev. Lett.* **109**, 032505 (2012).
- [7] A. Gando *et al.*, *Phys. Rev. Lett.* **110**, 062502 (2013).
- [8] T.R. Rodriguez and G. Martinez-Pinedo, *Phys. Rev. Lett.* **105**, 252503 (2010).
- [9] J. Menendez *et al.*, *Nucl. Phys. A* **818**, 139 (2009).

- [10] J. Barea and F. Iachello, *Phys. Rev. C* **79**, 044301 (2009).
- [11] F. Simkovic *et al.*, *Phys. Rev. C* **79**, 055501 (2009).
- [12] A. Staudt, K. Muto and H. V. Klapdor-Kleingrothaus, *Europhys. Lett* **13**, 31 (1990).
- [13] H.V. Klapdor-Kleingrothaus and I.V. Krivosheina, *Mod. Phys. Lett. A* **21**, 1547 (2006).
- [14] M. Agostini *et al.* *Phys. Rev. Lett.* **111**, 122503 (2013)
- [15] J.B. Albert *et al.* arXiv:1402.6956 [nucl-ex].